Available online at www.sciencedirect.com
ScienceDirect
Journal of Colloid and Interface Science 313 (2007) 232–247
JOURNAL OF Colloid and Interface Science
www.elsevier.com/locate/jcis

Catalytic effects on methanol oxidation produced by cathodization of platinum electrodes

Verónica Díaz [a], Carlos F. Zinola [b,*]

[a] *Chemical Engineering Institute, School of Engineering, J. Herrera y Reissig 565, C.P. 11300, Universidad de la República, Montevideo, Uruguay*
[b] *Fundamental Electrochemistry Laboratory, School of Sciences, Iguá 4225, C.P. 11400, Universidad de la República, Montevideo, Uruguay*

Received 21 December 2006; accepted 3 April 2007
Available online 31 May 2007

Abstract

A catalytic effect is found for methanol oxidation after new active surface states are produced on polycrystalline platinum by potentiostatic cathodization in acid media at room temperature. This procedure originates surface states not available on the original polycrystalline electrodes with unexpected cyclic voltammetric responses; i.e., at least four new peaks below 0.9 V are observed. The cathodization process also induces a rearrangement of the bulk platinum oxide, showing a defined peak at 1.2 V. The appearance of these new states is also proven by open-circuit potential decays. The electrocatalytic activity of these new surfaces in methanol oxidation is compared with that of the untreated electrodes by electrochemical impedance spectroscopy, chronoamperometry, and cyclic voltammetry. The cathodic procedure enhances the methanol oxidation voltammetric current peaks with charge density values higher than those on untreated platinum. The integration of chronoamperometric plots over 10 min in methanol acid media presents the largest difference between 0.6 and 0.7 V with respect to the original surface. Analysis of the impedance data shows that the values of polarization resistance for methanol oxidation on the cathodically treated platinum are lower than those of the original surface. According to the time constant values for methanol oxidation, the original surface can be considered less tolerant of the formation of catalytic poisons. A discussion of the most likely mechanism for the formation of the new active sites on platinum is presented here, assuming the presence of hydrogen subsurface states, ordered water clusters, and low-coordinated platinum atoms.

Keywords: Electrocatalysis; Platinum; Methanol; Subsurface hydrogen; Ordered water

1. Introduction

1.1. General aspects of platinum and platinum oxide electrochemical responses

The fundamental electrochemistry of platinum in aqueous media has been extensively studied under different experimental conditions by a number of diverse techniques [1,2]. Initial submonolayer stages of oxide film formation on single crystals (sc's) are characterized by a two-dimensional surface process. The geometry of the underlying platinum surface changes with respect to that of the initial oxide-free surface [2], however, remains essentially unaffected during further bulk oxide formation. The resulting structures are different from one another and from that of polycrystalline (pc) platinum.

On the other hand, the accepted mechanism of platinum oxide formation in aqueous solutions is not precise, since it ignores the history and pretreatment of platinum [3]. The formation of hydrous platinum oxides changes the normal voltammetric response, since a new metastable phase is formed. The oxygen-containing monolayer of Pt(II) species preceding Pt(IV) oxide formation is converted near the passive film to a single oxide modified by the place exchange mechanism, which partially stabilizes the electrode surface [3]. Hydrous metal oxides (β-oxides) are believed to be low-density materials with characteristics similar to those of structural water on the metal [3,4], that is, a refractive index similar to that of water. The growth and reduction of platinum oxides has been studied using a quartz crystal microbalance [5]. The compact α-oxide

* Corresponding author.
E-mail address: fzinola@fcien.edu.uy (C.F. Zinola).

0021-9797/$ – see front matter
doi:10.1016/j.jcis.2007.04.006

is anhydrous in nature (either PtO or PtO_2, depending on the applied potential), whereas the hydrous β-oxide films are consistent with a $PtO(OH)_2$ film composition [5]. Otherwise, in alkaline solutions [6], all α-oxides on pc platinum are nonhydrated even when a thick β-oxide film covers it (suggested to be $PtO_2{\cdot}H_2O$ [6]).

The effects of surface pretreatments change the morphological properties of platinum and its oxides. The annealing time affects the structural characteristics of amorphous platinum oxide thin films [7] and also the presence of oxygen in the decomposition of α-PtO_x [8]. Many studies have been performed for platinum thin films, which show their strong dependence on the surface free energy of each substrate [9–11]. Platinum layers of controlled roughness are grown by defined annealing and etching processes [12] and from the application of different electrode potential programs in strong acid or alkaline solutions [13,14]. Crystalline orientations can be obtained using fast repetitive potential signals through a mechanism of platinum faceting, which obeys a pulsating diffusion layer condition for the dissolution and redeposition processes [13,14]. Different types and morphologies of platinum oxides can be formed depending on the experimental conditions (symmetry of the wave, upper and lower potentials, frequency, and electrolyte).

On the other hand, three energy-degenerated PtO_2 phases were also found under UHV conditions [15]: a PtO_2 α-phase and β-phases at low and high oxygen pressures, respectively. Though never thermodynamically favored, the β-structure represents an appreciable fraction of the PtO_2 sample. However, there is increasing evidence from surface-enhanced Raman spectroscopy that the behavior of platinum/aqueous solution interfaces is more complex than is generally realized [16]. It was shown that the lattice energy in the outer layers of the metal might be reduced by severe cathodic or thermal pretreatments, exhibiting a complete different electrochemical profile of the interface [16].

1.2. On the formation of new active sites and oxide precursors at the platinum/aqueous interface

As pointed out above, metal surfaces can be activated by potential or thermal pretreatments, producing some new active centers on the surface [17,18]. The term "superactive" has been used by Burke [17,18] to denote an unusually active, metastable state that undergoes oxidation at potentials lower than expected [16]. The basis of this new surface state has been discussed, along with its importance in electrocatalysis [17–20]. The new anodic response at 0.25 V [17] is observed only when thermally activated electrodes are subjected to additional activation using cathodic polarization. The role of such active atoms produced by cathodization and their preoxidation products, named incipient oxide species, is as mediators in electrocatalysis of anodic processes. These incipient oxides have been proposed [21] as nonequilibrium metal surface states produced after exposure to the electrolyte [22]. Furthermore, Frumkin has reported double-layer capacities for platinum/solution interfaces ranging from 15 to 50 $\mu F\,cm^{-2}$ [23], attributing the differences to anion adsorption and reactions of hydrogen or oxygen species occluded in the metal. Similar features have been observed [24,25] when platinum is polarized in hot concentrated phosphoric acid. Equivalent effects are found for platinum films oxidized at high temperatures in the presence of oxygen (back spillover), i.e., a reversible oxide (PtO_x) and two strongly irreversible oxides [26].

1.3. Changes in the electrocatalytic behavior of the platinum/aqueous interface

Platinum metal dispersion preparation methods have been used to study several reactions [27]. The effect of electrochemical promotion on catalytic activity has been investigated on these surfaces [28], taking the complete oxidation of ethylene as a model reaction. It is found that the catalytic rate can be reversibly enhanced by a factor of 5 through the application of a potential program on platinum catalysts. This increase has been assigned to the electrochemical migration of anionic oxygen between the electrolyte and the metal [28]. Electrochemical modifications on surfaces have been also analyzed for the complete oxidation of propane on porous platinum in the temperature range 425–520 °C. Application of either positive or negative overpotentials resulted in nonfaradaic increase of the catalytic rate, by up to a factor of 1350 on platinum [29]. However, the oxygen reduction kinetics [30] exhibits a strong inhibition in alkaline solution when the electrodes have different thickness of hydrous platinum oxides.

Classically, the increase of the platinum electrocatalytic performance toward anodic reactions can be achieved by including a second (or a third) metal [31–40]. Promising results have also been obtained using spontaneous deposition [41–48], mostly with ruthenium and tin. All platinum-decorated samples yielded large catalytic activities for methanol oxidation at potentials of interest for fuel cells [49]. In avoiding the poisoning of the platinum anode catalysts [50–52], the new platinum materials PtRu and PtSn exhibit good results [52], but some of them have shown contradictory results. Hable and Wrighton [53] have found that methanol oxidation on PtSn and PtRu electrodeposited on polymers perform better on ruthenium than on a tin-containing catalyst. Wang et al. [54] have shown an increase in methanol oxidation on a sputtered $Pt_3Sn(110)$ surface, but smaller than that observed on PtRu alloys. Napporn et al. [55] report that highly dispersed PtSn electrodes could be as active as PtRu for methanol oxidation, but this depends on the method of PtSn preparation. Morimoto and Yeager [56] have studied methanol electrooxidation on ruthenium and tin electrodeposited on smooth or platinized platinum. On the smooth surface, ruthenium promotes catalytic activity according to the surface coverage, while tin shows a good effect only for a short period of time (due to tin dissolution). However, on platinized platinum, tin is stable and exhibits effects as long-lasting as those of ruthenium-containing catalysts. The study of methanol oxidation on Pb/Pt electrodes [57] modified by a thin film of poly(*o*-phenylenediamine) with electrodeposited Pt, PtRu, and PtSn has demonstrated that dispersed Pt–Sn prepared under pre-

cise conditions is more active than Pt and Pt–Ru. Kobayashi and co-workers [58] observe that electrocatalytic methanol oxidation over PtRuSn/C ternary alloy (Pt:Ru:Sn atomic ratio of 50:33:17) is higher than that of PtRu/C and PtSn/C with atomic ratio 50:50. Recently, it has been shown that PtSn/C electrocatalyst prepared by the alcohol reduction process is more active than PtRu/C and PtSnRu/C electrocatalysts for methanol oxidation [59]. The better performance was ascribed to the fact that only part of tin was found as a PtSn alloy, which changes the platinum's electronic properties, while the rest, found as SnO_2, assists the oxidation of adsorbed carbon monoxide intermediate. The problem of Pt/Ru or Pt/Sn nanoparticle size in the electrocatalysts is important in lowering the catalyst loading in anodes for methanol electrooxidation. The size of the Pt–Ru/C nanoparticles can be lowered down to 4.3 nm and the activity maintained [60]. The stability of Pt–Ru/C nanoparticles prepared in alkaline solutions is higher than that for the other solutions due to the citrate complexation stabilizing effect.

The application of electrochemical or thermal pretreatments has shown its importance in electrocatalysis [16,17]. New interesting improvements in low-chained organic fuels oxidation have been found on different metal surfaces [17–20]. However, the extent of the effect and the mechanism of the process are not yet well understood. In order to improve activity and stability of dispersed catalysts, they can be heated at high temperatures. The optimal heat-treatment temperature has to be scanned to check the average particle size of the metal catalyst. These methods were assayed for synthesized Pd–Co/C catalyst [61]. Well-dispersed platinum nanoparticles with controlled size distribution can be prepared by polyalcohol reduction of platinum salts, using capping agents [62]. The particles have to be activated for electrocatalytic heating in air at 185 °C for 5 h, conditions that gave no particle sintering and no oxidation. The smaller 3.5-nm platinum particles have a higher intrinsic activity for methanol oxidation, but a lower tolerance of carbon monoxide poisoning, compared to particles of 6.0–11.5 nm. The enhancement of methanol oxidation has been also found in other papers [63]. Electrochemical measurements demonstrated that the PtRu/C catalysts obtained with sensitizing and activating pretreatment exhibited an enhanced peak current density of 34% for methanol electrooxidation as compared to that synthesized without pretreatment. Multiple combinations of noble and non-noble metals have been assayed to check the methanol oxidation catalysis, with promising results [64–66].

These findings lead us to continue looking for a better catalyst for methanol oxidation, without the inclusion of another metal, using the concept of the surface oxidation of methanol intermediates with water-discharged products. Since the oxidation of organic surface species on platinum entails the mediation of appropriate oxygen-containing adsorbates, premonolayer oxidation on new active sites can be promised to catalytic purposes. In this work, it has been found that the application of a potential perturbation in the true hydrogen evolution region produces a new platinum morphology with new current vs potential profiles in the range from 0.5 to 0.75 V with catalytic activity in methanol electrooxidation.

2. Experimental

Electrochemical runs were performed using a three-electrode compartment cell with a pc platinum wire as a working electrode of different geometric areas from 0.5 to 4 cm^2 (99.999% purity, from Goodfellow). For comparative purposes a Pt(111) sc (0.5 cm diameter, 99.998% purity, and cut ±0.5°, from Metal Crystals & Oxides) was used, which was prepared as explained before [67] and mounted in the cell using the dipping technique under a nitrogen atmosphere [68].

A large-area smooth platinum counterelectrode and a reversible hydrogen reference electrode with a Luggin–Haber capillary tip completed the electrochemical system. Potential values in the text are given on the hydrogen reference electrode (RHE) scale. As supporting electrolyte, 1 M sulfuric acid (96–98% analytical reactive from Baker) was employed, which was prepared using ultrapure water from Millipore-MilliQ plus (resistivity 18.2 MΩ cm).

The cathodization method (CT) implies the application of a constant potential (E) from −2 to 0 V for a certain time from 5 to 60 min in the supporting electrolyte. The current transients were recorded during the process and a potentiostatic holding at 0.05 V for 10 min was applied to eliminate dissolved molecular hydrogen under continuous nitrogen bubbling. Immediately after and under continuous potential control, either the cyclic voltammograms from 0.05 to 1.55 V, run at 0.10 V s^{-1}, or the open-circuit potential transients were performed. The stability of the new surfaces was studied by the latter methodology in the supporting electrolyte for a given time. The platinum real area before and after the pretreatments was calculated from the integration of the hydrogen adatom voltammetric profile (after double-layer correction). All runs were achieved at 20 ± 2 °C, under free oxygen conditions using nitrogen (99.998% purity).

In order to study the electrocatalytic performance of the new surfaces produced by the CT, three methodologies were conducted in oxygen-free 0.1 M methanol + 1 M sulfuric media, namely, linear sweep voltammetry, chronoamperometric transients, and electrochemical (potentiostatic) impedance spectroscopy. Linear sweep voltammetry was conducted on each surface, starting from 0.20 V and scanning toward positive values at 0.10 V s^{-1}. The charge densities under the main anodic peak were also calculated. Chronoamperometric curves were performed for 20 min at the same potentials of the impedance spectra (from 0.250 to 0.775 V). The charge density values under the chronoamperometric plots were calculated for 10 min for comparison purposes only. The impedance spectrum was performed at constant potential in the range 0.1–10^5 Hz, taking 10 points per decade.

The electrochemical experiments were performed using a PGZ 301 Voltalab potentiostat–galvanostat–impedance using the Voltamaster 4 software with homemade electrode and cells.

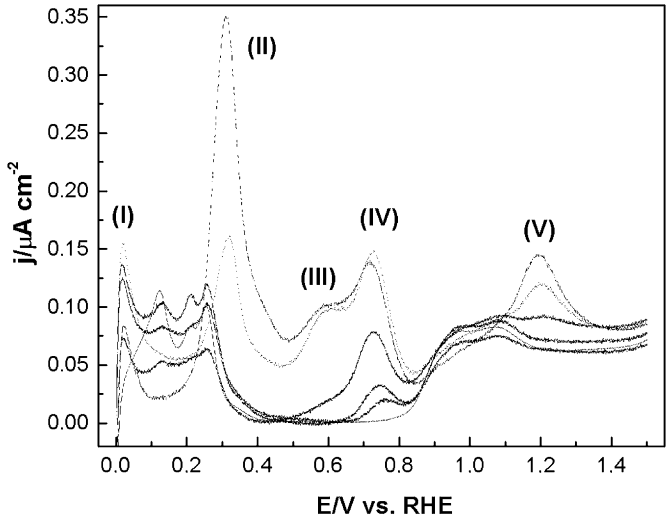

Fig. 1. First positive-going potential profile of pc platinum (solid line) runs between 0.05 and 1.55 V at 0.10 V s^{-1} in oxygen-free 1 M sulfuric acid solution. The CT is applied for 5 min at $E = -0.5$ V (gray line), $E = -1.0$ V (light gray line), $E = -1.5$ V (dotted line), and $E = -2.0$ V (dashed line).

3. Results and analysis

3.1. Cathodic pretreatments on platinum in acid media

3.1.1. Cyclic voltammetric runs for CT platinum in acid media

The initial positive-going potential sweep, after the CT is applied at different E values for 5 min using a smooth large-area counterelectrode, is shown in Fig. 1. In comparison with untreated electrodes, the CTs lead to unusual cyclic voltammetric responses. Five different peaks were observed in the voltammogram at ca. 0.05, 0.32, 0.65, 0.75, and 1.20 V (identified by roman numerals). These peaks are related to the formation of new active sites emerging from the net hydrogen evolution process developed on the platinum crystal lattice. Peak currents and charge densities increase with the absolute value of E. There was a tendency to return to the electrochemical behavior of a normal cyclic voltammetric response during subsequent cycles (increasing with the value of E). However, in the case of the range 0.5–0.75 V, more than 50 cycles are required to obtain the original current vs potential profile of the unperturbed platinum. This is an important feature because the formation of the new surface morphology is stable upon potential cycling, especially at long-lasting polarizations. Thus, its use in electrocatalysis can be envisaged as promising.

The new features compared to the typical voltammetric response of an untreated platinum electrode are reproducible. Three distinct regions can be defined in the first positive potential incursion. The first region (from 0.05 to 0.40 V) shows one peak (I) at 0.05 V, which is simply ascribed to traces of molecular hydrogen oxidation not eliminated at 0.05 V after the CT. However, one of the most interesting features is the enhancement of the "third anodic peak" at ca. 0.2 V. The origin of this peak is controversial and is attributed to the formation of subsurface hydrogen [69] or to incipient hydrous oxide species [20]. We have observed the rearrangement of hydrogen adatoms toward strongly adsorbed hydrogen after a potentiostatic holding in the range 0.03–0.09 V [69]. However, for E values lower than 0 V, the hydrogen desorption region became partially inhibited and a large anodic peak (II) can be observed at ca. 0.32 V. This peak partially disappears when the solution is stirred and only 30% of the anodic contribution is still observed. Thus, different situations can be inferred: the formation of platinum soluble species, desorption of subsurface hydrogen from new active sites, and crystal lattice restructuring. The adsorption of hydroxyl species at these very low potentials is rejected since the working electrodes are not sc surfaces.

Table 1
Peak potential (E_{peak}) and anodic charge densities (σ_{peak}) for the voltammetric profile of CT applied for 5 min on platinum as a function of E in 1 M sulfuric acid solution

E (V) in CT	Peak number	E_{peak} (V)	σ (μC cm^{-2})
0	IV	0.76	21
−0.5	IV	0.74	39
−1.0	III	0.60	28
−1.0	IV	0.73	102
−1.0	V	1.21	12
−1.5	II	0.32	218
−1.5	III	0.65	147
−1.5	IV	0.73	199
−1.5	V	1.19	105
−2.0	II	0.31	426
−2.0	III	0.64	149
−2.0	IV	0.72	182
−2.0	V	1.19	140

On the other hand, the electrochemical response after the CT procedure also extends to the second region, that is, the double-layer charging/discharging domain (from 0.5 to 0.8 V). Instead of the flat pseudo-capacitance response, two adjacent peaks can be seen at ca. 0.65 and 0.75 V (peaks III and IV). These peaks are rather stable upon successive potential cycling, so special attention is paid to them. The electrochemical response in the third region (from 0.80 to 1.50 V) is also interesting since a new peak (V) at 1.20 V is originated when a characteristic CT is applied. This effect has been observed before on sputtered platinum–Teflon membranes prepared for DEMS experiments [70]. A partially inhibited platinum oxide is observed (as in Fig. 1) between 0.9 and 1.0 V with charge densities lower than those on original platinum. The lower charge is compensated for by the appearance of a broad peak (V) at 1.20 V. The effect is similar to surface blocking by strongly bound anions, but in this case, platinum oxide reconstruction can be postulated, as previously observed for the DEMS setup.

Table 1 illustrates the peak potentials and charge densities to characterize the process at different E values. Peak (I) is difficult to integrate because of the different baseline currents, but in all surfaces lies at ca. 10–50 μC cm^{-2}. It is worth noticing that the charges under peak (II) are rather large (more than a monolayer) and are strongly dependent on the E value and the time of

Table 2
Peak potentials (E_{peak}) and peak current densities (j_{peak}) for peaks (III) and (IV) and charge densities (σ_{peak}) within the potential range 0.45–0.86 V as a function of E applied for 5 min on platinum in 1 M sulfuric acid solution

E (V)	$E_{peak\ III}$ (V)	$E_{peak\ IV}$ (V)	$j_{peak\ III}$ (mA cm^{-2})	$j_{peak\ IV}$ (mA cm^{-2})	$\sigma_{peak\ III–IV}$ (μC cm^{-2})
0	–	0.76	–	0.02	21
−0.5	–	0.74	–	0.033	39
−1.0	0.60	0.73	0.02	0.079	130
−1.5	0.65	0.73	0.10	0.148	346
−2.0	0.64	0.72	0.11	0.140	332

the CT. For example, for $E = -2$ V (and 5 min) the charge density reaches 426 μC cm^{-2}. Charge densities under peaks (III) and (IV), when E values are more negative than −1.5 V, remain practically constant at 340 μC cm^{-2}. On the other hand, the intensity of peak (V) increases for more negative values of E, reaching 290 μC cm^{-2} for $E = -2$ V.

The region interesting for electrocatalysis of anodic processes is that from 0.45 to 0.86 V. The charge densities under the addition of both peaks (III) and (IV) are figured in Table 2 as a function of E. No further changes in the peak potential values (0.64 and 0.72 V) for the two peaks are observed with E values lower than −1.5 V. Also, the equilibrium charge density (ca. 340 μC cm^{-2}) shows that the appearance of these new features (induced by the CT) reaches some kind of saturation. This fact illustrates that the platinum surface is the determining step of the entire process.

Since we have decided to show only the relevant features observed after performing the CT, Fig. 1 does not exhibit the negative potential sweep response of platinum. In cycling up to 1.5 V, the normal repetitive cyclic voltammetry of platinum oxide reduction in sulfuric solution is observed. But when cycling up to not more than 1 V, a cathodic counterpeak at ca. 0.5 V is observed, which is why we decided to perform potential window experiments.

When the CT is applied in acid solution and the supporting electrolyte is subsequently exchanged with base (pH 12), the profile does not show any new information as compared to the same CT process applied directly in base. No new features comparable to those observed in sulfuric acid developed, even when long-lasting experiments (more than 1 h) were performed. The problem of the instability of the CT platinum in aqueous solution upon transfer to a new cell, or after exchange of the solution under a microflux cell, has been also proven. Thus, the cathodization effect only takes place at the interface, probably producing a highly ordered water (or hydroxyl) overlayer on new platinum sites. Only a small charge density previous to the normal platinum oxide formation is observed when the electrolyte is exchanged with a fresh acid solution (previously named peak (IV) in Fig. 1).

Since we are interested in the catalytic performance of the new platinum surface, we have performed some potential window experiments to get some light into the CT process (Fig. 2). The effect of potential cycling was studied covering only the range 0.05–0.90 V, after the CT was applied at $E = -1$ V for 15 min without changing the base electrolyte. Fig. 2 shows the

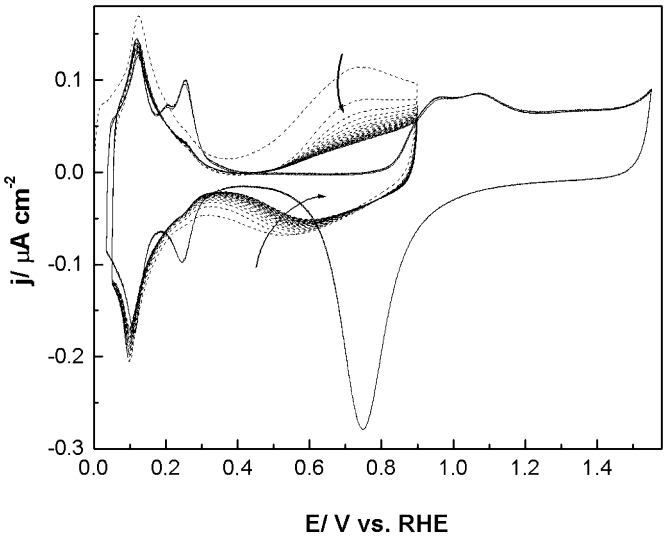

Fig. 2. Potential window profiles for CT platinum (dashed line) run between 0.05 and 0.90 V at 0.10 V s^{-1} in oxygen-free 1 M sulfuric acid solution at room temperature. The CT is applied at $E = -1.0$ V for 60 min. The cyclic voltammetry of untreated platinum is run between 0.05 and 1.55 V (solid line).

formation of a quasi-reversible couple with anodic and cathodic peak potentials lying at 0.72 and 0.52 V, respectively. Subsequent and multiple potential cycling up to 0.90 V produces a decrease of the redox couple currents until a stable system is achieved (more than 100 cycles). In the hydrogen adsorption region it is clearly seen that the strongly bound hydrogen adatom is totally suppressed even at the end of the cycles. However, the weakly bound hydrogen adatom remains stable upon potential cycling. No increase in the surface area is observed. It is likely that the presence of the redox couple is the result of water discharge at lower potentials producing some kind of hydroxyl species on new platinum active sites. The inhibition of the strongly bound hydrogen suggests a change in the crystalline structure of platinum or its morphology to a more disordered surface, which is not able to adsorb this type of hydrogen adatom. These facts will be used later in Section 4. It is also important to mention that when the same potential window experiment is performed, but for briefer experiments (less than 5 min) or with continuous nitrogen bubbling in the supporting electrolyte, the negative-going potential scan experiments show a reactivation and the current contour practically coincides with that of the positive-going potential sweep direction. This means that the formation of soluble or, more properly, hydroxyl or water partially discharged products at the platinum interface is responsible for the cyclic voltammogram depicted in Fig. 2.

3.1.2. Open-circuit potential decays for CT-treated platinum in acid media

We have performed chronopotentiometric curves at zero current (open-circuit potential decays) to study the stability of the new platinum morphologies obtained by the application of the CT method. We only check those surfaces prepared using $E = -1$ V for different times ranging from 5 to 60 min without changing the supporting electrolyte. Fig. 3a shows that

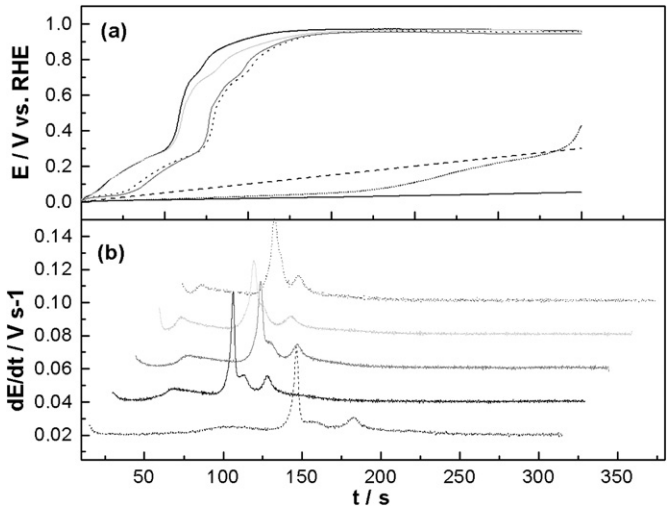

Fig. 3. (a) Open-circuit potential and (b) first derivative decays on CT platinum with $E = -1$ V in oxygen-free 1 M sulfuric acid for 5 min (continuous line), 10 min (light gray line), 15 min (dark gray line), 20 min (dotted line), 30 min (dashed line), 45 min (short dotted line), and 60 min (gray line).

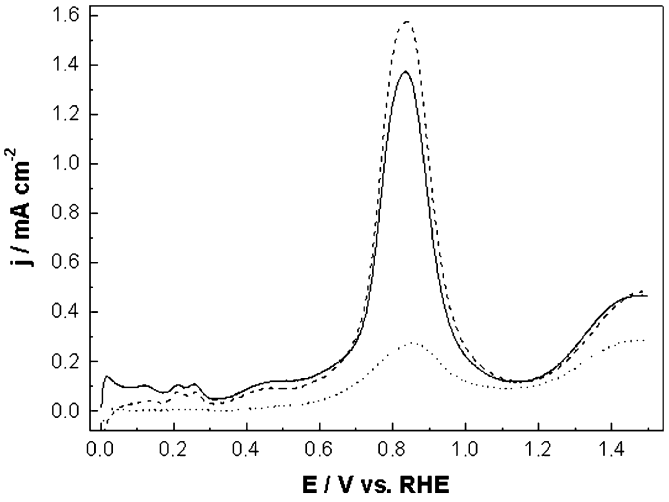

Fig. 4. First positive-going potential scan for methanol electrooxidation run between 0.05 and 1.55 V at 0.10 V s^{-1} in oxygen-free 0.1 M methanol + 1 M sulfuric acid solution at room temperature; untreated platinum (solid line), CT prepared at $E = -1.0$ V for 5 min in sulfuric solution (dashed line), CT at $E = -1.0$ V for 5 min applied in methanol solution (dotted line).

nearly the same potential decay profile is obtained independent of the CT time. At least three potential jumps, from 0.05 to 0.28 V, from 0.30 to 0.68 V, and from 0.70 to 0.98 V, are observed. A limiting stable potential value is attained at ca. 1 V. This value is different from the common open-circuit potential (0.84–0.88 V) of pc platinum in sulfuric acid in oxygen-free solution. The time at which the open-circuit potential plateau is reached depends on the interval of time in which E was applied during the CT. When the CT is applied for 5 to 20 min, the constant open-circuit value of platinum is reached after 150 s (Fig. 3a). However, for 60 min of CT, there is a higher stability of the new surface, since it attains a plateau after 1350 s (not shown). Hoare [71] has shown that large values of open-circuit potentials can be observed when derm-adsorbed oxygen is prepared after very long-lasting anodization on platinum. Our results showed, then, that the saturation value of ca. 1 V indicates the presence of some type of oxygen-containing species on platinum.

Sometimes it is better to evaluate the chronopotentiometric curve as its first derivative (Fig. 3b), where the different potential jumps are better seen as peaks. We could say that each peak would correspond to a new state in the platinum surface morphology. Again, at least three peaks (each of them with a second hump) can be defined, corresponding to peaks (II), (III), and (IV) of the linear sweep voltammetry in Fig. 1. This kind of behavior is only seen when a true new stable species or phase is formed on the surface. It is important to say that after the open-circuit potential decays were completed, cyclic voltammetry could be performed to check for some electrochemical feature still present on the surface. The first cathodic incursion down to 0.05 V and the subsequent anodic incursion still showed the presence of peaks (III) and (IV) for more than a dozen cycles. This means that the ca. 1 V of open-circuit potential is probably a consequence of producing subsurface hydroxyl species.

3.2. Electrocatalytic performance of untreated and CT electrodes in methanol oxidation

3.2.1. Linear sweep voltammetric runs in methanol acid media

The first positive-going potential scans starting from 0.2 V for methanol electrooxidation on pc and CT platinum in 0.1 M methanol + 1 M sulfuric acid media are shown in Fig. 4. Two main situations were considered: the application of CT at $E = -1.0$ V either in 1 M sulfuric solution or in methanol acid solutions. It is possible to observe larger current densities when the CT is applied in the supporting electrolyte than in a methanol-containing solution. In fact, the result of the latter is the inhibition of the reaction due to poisoning by adsorbed carbon monoxide formed from methanol intermediates. At low potentials, some type of adsorbed intermediate, oxidatively removed from ca. 0.5 V, deactivates the surface. A maximum current density is observed at ca. 0.85 V, above which the rate of methanol oxidation decreases due to platinum oxide formation (which also deactivates the surface). After the oxide is reduced during the negative-potential sweep, methanol oxidation current starts at ca. 0.9 V (not shown). However, this response decays from 0.6 V as a consequence of adsorbed carbon monoxide species.

After the CT procedure was applied in acid solution, the peak current density was 15% greater than that obtained on the untreated electrode. The electrocatalytic activity was enhanced even after several cycles; in particular, in the fifth cycle (not shown), a relative difference in the peak current density of 26% between the CT and the original electrode was observed. A small prewave in the methanol oxidation profile is observed in the range 0.30–0.60 V, which has different relative components on CT and untreated surfaces. The lower contribution observed for the treated surfaces indicates smaller coverage by disordered carbon monoxide adsorbates, which seems to be related to the larger peak currents observed for this surface in Fig. 4.

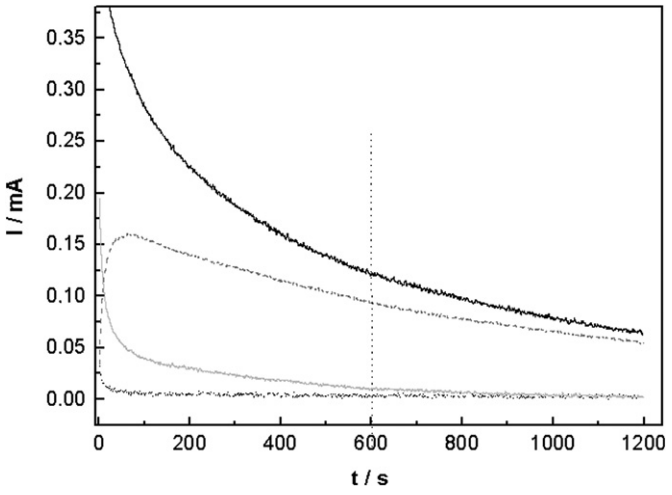

Fig. 5. Chronoamperometric transients for methanol oxidation in oxygen-free 0.10 M methanol + 1 M sulfuric acid recorded at 0.65 and 0.725 V on untreated platinum (dotted and gray lines, respectively) and on CT platinum (light gray and black solid lines, respectively). The CT was applied at $E = -1.0$ V for 5 min in sulfuric acid solution.

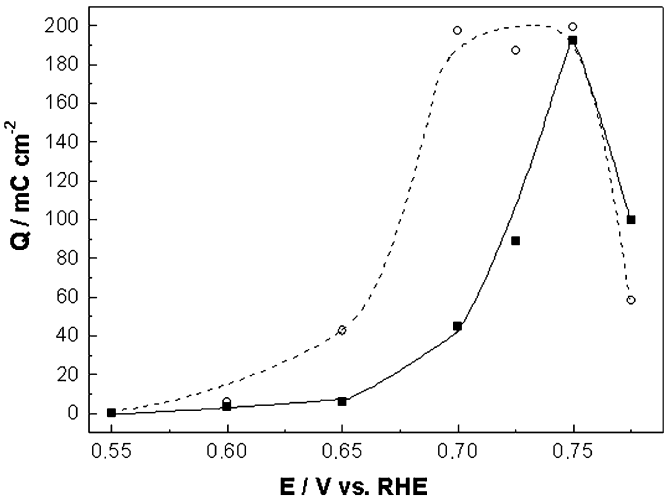

Fig. 6. Chronoamperometric charge density vs applied potential evaluated at 10 min for untreated pc platinum (■) and CT at $E = -1.0$ V applied for 5 min in sulfuric acid solution (○) in oxygen-free 0.1 M methanol + 1 M sulfuric acid solution at room temperature.

3.2.2. Chronoamperometric plots in methanol acid media

Chronoamperometric curves were run for methanol oxidation on the CT surfaces (for $E = -1$ V during 5 min) under different constant potentials ranged from 0.250 to 0.775 V. Fig. 5 shows only the 0.65- and 0.725-V current density transients until 20 min. Both surfaces usually illustrate a typical diffusion-controlled decay, but at potentials higher than 0.7 V, pc surfaces exhibit a first current increase at very short times. This fact is the result of a competitive process between carbon monoxide and adsorbed methanol oxidations. The pc platinum seems to be poisoned by a greater extent of carbon monoxide adsorbates. This effect is not observed at low potentials.

The charge density at a fixed potential found under the chronoamperometric transients evidenced the real electrocatalytic activity of the surface. Fig. 6 represents the integration of the charge until 10 min as a comparison of treated and untreated electrodes as a function of the potential. At 0.65 V, methanol oxidation did show a current contribution on the CT surface, not distinguished on the other surface. For potentials below 0.75 V, the charge densities found on the CT surface are always higher than those of treated platinum, for example, 200 mC cm^{-2} at 0.7 V. At this potential, it is possible to perceive the largest difference between each type of surface, with charge density values 340% higher than those on original platinum. Charge density values between 0.675 and 0.775 V on CT platinum are nearly the same (200 mC cm^{-2}). This effect can be associated with the development of an electrochemical couple (shown earlier in Fig. 2) that is responsible for the catalytic performance of methanol oxidation previously observed as peaks (III) and (IV) in Fig. 1.

In the case of the pc untreated platinum, the maximum charge density is obtained at 0.75 V (192 mC cm^{-2}), i.e., at a higher potential. This means that the CT produces a deeper perturbation at the platinum/acid solution interface, which activates the surface for methanol oxidation reaction at lower potentials. However, at a characteristic potential, the two types of surfaces exhibit similar charge densities; a smaller value for CT surfaces was even reported for 0.775 V. It is possible that two competitive effects occur during the process: methanol oxidation in solution and the leakage of the surface generated by the CT. All results presented in Fig. 6 were normalized to the initial untreated electrode area, as said before.

3.2.3. Electrochemical impedance spectroscopy in methanol acid media

After 20 min of potential holding, electrochemical impedance spectra were performed and the results fitted according to the usual equivalent circuits. The Randless model, R_s (R_pCPE) was used in the potential range 0.55–0.775 V and the R_sCPE model in the range 0.25–0.40 V, R_s, R_p, and CPE being the solution resistance, polarization resistance, and constant phase element, respectively. Goodness of fit was evaluated by the statistic value chi-squared.

The Nyquist diagram performed at 0.725 V is presented in Fig. 7 for untreated and CT platinum prepared with $E = -1$ V for 5 min. In a simple view, the impedance data plotted in the complex plane do not reveal any complementary effects as second semicircles due to experimental constraints on the frequency range. However, in the inset of the figure, a tendency to form a second semicircle from 25 to 6.3 kHz can be seen, besides the expected tendency at lower frequencies. These two semicircles may be ascribed to charge-transfer processes, since diffusion effects are not observed for the methanol concentrations used in this paper. Several derivations for the impedance of such reactions were previously reported [72], in which two semicircles in the impedance plot implied a reaction with one adsorbed intermediate.

The fitting of R_p and CPE parameters from the equivalent circuit are plotted in Figs. 8a and 8b as a function of the electrode potential. These values are taken as the kinetic parameters of the potentiostatic methanol oxidation. A close examination of the high-frequency data (at potentials higher than 0.5 V) re-

vealed electrode potential independence of the impedance data between 5 kHz and 5 Hz, suggesting a charge-transfer process at the outermost layer of platinum. To consider the physical significance of the CPE element, we are going to make some assumptions, as explained below.

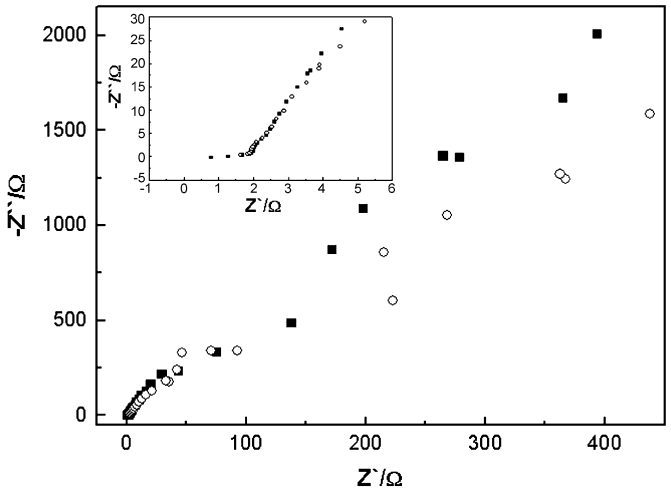

Fig. 7. Nyquist diagram for methanol oxidation at 0.725 V on (■) pc platinum; (○) platinum pretreated with CT at $E = -1$ V for 5 min in 1 M sulfuric acid solution. The inset shows a Nyquist diagram for methanol oxidation at 0.725 V between 25 and 6.3 kHz.

In the absence of charge-transfer processes; the behavior of the interface can be modeled as an R_sCPE circuit, whose impedance, Z, can be calculated according to

$$Z = R_s + (i\omega)^{-(1-\alpha)}Q, \tag{1}$$

where R_s is the resistive limit of Z at infinite frequencies, Q is a constant related to the CPE with $\Omega\,s^{-(1-\alpha)}$ dimensions, and α is related to the rotation angle (between 0 and 1). Considering the time constant, τ, of this RC circuit, we can simply ascribe the CPE to a double-layer capacitance C_{dl} when no frequency dependence is observed:

$$\tau = R_s C_{dl}. \tag{2}$$

Then, Z will be [72,73]

$$Z = R_s\left[1 + (i\omega\tau)^{-(1-\alpha)}\right]. \tag{3}$$

When the C_{dl} depends on the applied frequency, after comparing Eqs. (1) and (3), we can select C_0 as the frequency-dependent capacitance of the double layer:

$$C_0 = \left(Q^{-1}R_s^{\alpha}\right)^{1/1-\alpha}. \tag{4}$$

In the case of an irreversible charge-transfer process, we have the following value of the CPE according to Sluyters and co-workers [73],

$$Q = C_0^{\alpha}\left[R_s^{-1} + R_p^{-1}\right]^{1-\alpha}, \tag{5}$$

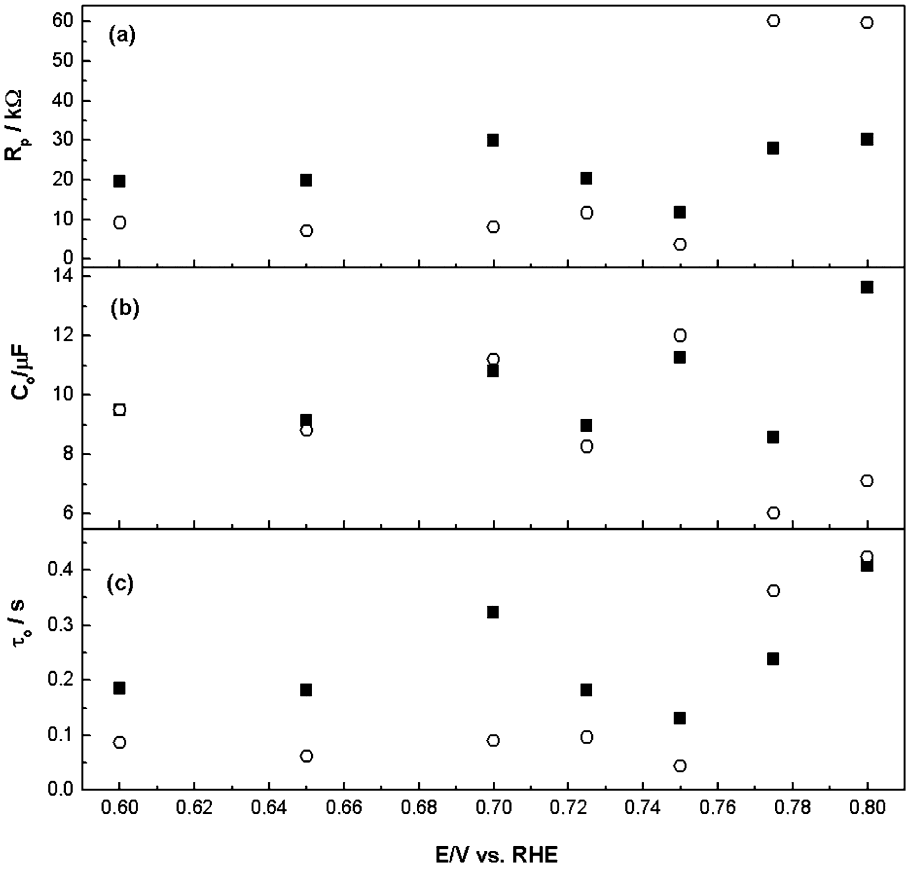

Fig. 8. (a) R_P polarization resistance, (b) C_0 double layer capacity, and (c) τ_0 time constant vs applied potential for methanol oxidation on untreated platinum (■) and CT at $E = -1.0$ V for 5 min in 1 M sulfuric solution (○).

where R_p being the polarization resistance of the methanol oxidation. It is clear that the CPE is coupled not only to R_s but also to R_p. We can again use the values of C_0 as representative of the CPE.

From the fitting of our experimental results it can be observed that R_s lies at 1.3 Ω. Moreover, the values of R_p (Fig. 8a) for the untreated platinum are higher than those obtained with the CT surfaces below 0.75 V. At potentials higher than 0.75 V, R_p values for CT platinum surfaces are almost threefold higher, a fact attributed to a lower rate due to carbon monoxide formation. It is important to point out that again, at 0.70 V (the potential at which the maximum difference between chronoamperometric charges is observed), R_p values are threefold lower than those obtained from untreated platinum (Fig. 8a). On the other hand, C_0 for the untreated and CT surfaces are similar, i.e., from 9 to 11 μF at potentials lower than 0.75 V (Fig. 8b). Above this potential, C_0 reaches higher values for the untreated surfaces. The circuit elements that contain information about methanol electrooxidation are R_p and C_0. The inverse of R_p describes the change of the rate for the methanol oxidation charge transfer with the electrode potential when the coverage of the intermediate is held constant [74],

$$R_p^{-1} = F\left(\frac{\partial \nu}{\partial E}\right)_\theta = F\left(\frac{\partial \nu}{\partial \theta}\right)_E \left(\frac{\partial \theta}{\partial E}\right)_\nu, \tag{6}$$

where F is the Faraday constant, ν is the rate of charge transfer in mol s^{-1} (at a constant working electrode area), E is the electrode potential, and θ is the coverage of the adsorbed intermediate on platinum. R_p^{-1} describes the potential dependence of the charge transfer rate constants. The value of $(\partial \nu/\partial \theta)_E$ decreases exponentially with the surface coverage by adsorbed carbon monoxide. Since R_p^{-1} is positive, it will also depend on $(\partial \theta/\partial E)_\nu$, so the latter derivative has to be negative. The values of θ decrease with the electrode potential, as in the course of the methanol oxidation reaction.

On the other hand, C_0 can be taken as

$$C_0 = \frac{F}{N_A}\left(\frac{\partial \theta}{\partial E}\right)_\nu = \frac{F}{N_A}\left(\frac{\partial \nu}{\partial E}\right)_\theta \left(\frac{\partial \nu}{\partial \theta}\right)_E^{-1}, \tag{7}$$

N_A being the Avogadro number. There is no significant variation of C_0 with the electrode potential until at least 0.75 V. Thus, since $(\partial \nu/\partial E)_\theta$ is equivalent to R_p^{-1}/F, it increases very little with the electrode potential until 0.75 V. As a consequence, the same has to observed on $(\partial \nu/\partial \theta)_E^{-1}$. In the case of a Langmuirian condition of coverage, we can say that C_0 is

$$C_0 = \frac{Q\delta F}{RT}\theta(1-\theta), \tag{8}$$

Q being the charge accumulated at the interface, δ the charge transfer by the adsorbed species, and the rest of the symbols having their usual meaning. The values of the reaction rate are rather buffered by the $\theta(1-\theta)$ condition, so no strong exponential dependences on θ are likely to occur. This situation accounts for when the presence of poisons at the surface is very little. For potentials higher than 0.75 V, CT platinum exhibits lower C_0 values than untreated platinum. This means that net faradaic processes such as methanol oxidation governed the current on untreated platinum. On the other hand, the restructuration of CT to "normal" platinum is probably occurring on the other surface, which exhibits capacitance behavior.

To take into account the effect of both C_0 and R_p, the time constant (τ_0) element is considered according to [73]

$$\tau_0 = \tau/\left(1 + R_s R_p^{-1}\right). \tag{9}$$

The τ_0 constant for methanol oxidation was calculated simply from the product of R_p and C_0 (R_s was omitted, since R_p^{-1} shows negligible values) and plotted in Fig. 8c. At potentials higher than 0.75 V, CT surfaces exhibits higher τ_0 values indicating higher specific rate constants for methanol oxidation. For example, at 0.775 V, τ_0 changes from 0.23 to 0.36 s for pc and CT platinum, respectively. In contrast, at lower potentials, the higher τ_0 values for untreated platinum (especially at 0.70 V) denote the dominance of the R_p component. The τ_0 dependence on θ obeys the formula

$$\tau_0 = \frac{1}{N_A}\left(\frac{\partial \theta}{\partial \nu}\right)_E = \frac{1}{N_A}\left(\frac{\partial \nu}{\partial E}\right)_\theta^{-1}\left(\frac{\partial E}{\partial \theta}\right)_\nu^{-1}. \tag{10}$$

The increase in τ_0 with the electrode potential is associated with lower $(\partial \nu/\partial \theta)_E$ values. This result indicates that the change in the oxidation rate with intermediate coverage is affected mainly by the electrode potential and not by coverage changes with the electrode potential. According to our results, the untreated surface can be considered as less tolerant of the formation of catalytic poisons. This means that the catalytic effect of the CT procedure can be attributed to a decrease in θ by intermediates of methanol oxidation.

4. Discussion

4.1. General features of the cathodization process on platinum

Our experimental results obtained by applying a CT in the true hydrogen evolution region were outlined above. The effects of the CT on the voltammetric profile of the platinum/acid interface are basically presented in Figs. 1 and 2 and are interpreted as the anodic potentiodynamic responses of new platinum surface rearrangements in aqueous solutions. As detailed in Fig. 1, the sudden increase in the current density (peak (I)) just after the potential scan is reversed is attributed to traces of molecular hydrogen oxidation. Peak (II) is rather difficult to analyze, since at last two features are involved during its formation. Since it partially disappears after the electrolyte is stirred, it might involve the oxidation of a soluble component together with the surface oxidation of some species arising from the cathodization. Considering that peak (II) persists on the surface by ca. 30% after the electrode is rotated at 500 rpm and the normal hydrogen adatom response (between 0.05 and 0.40 V) is totally observed during the first positive-going potential scan, the formation of a new hydrogen state, such as subsurface hydrogen or hydrogen adsorbed on a new active platinum center, is likely.

However, it is well known that the hydrogen evolution reaction at high negative potentials produces an increase of the pH at the interface on noble metals. Thus, the alkalinization

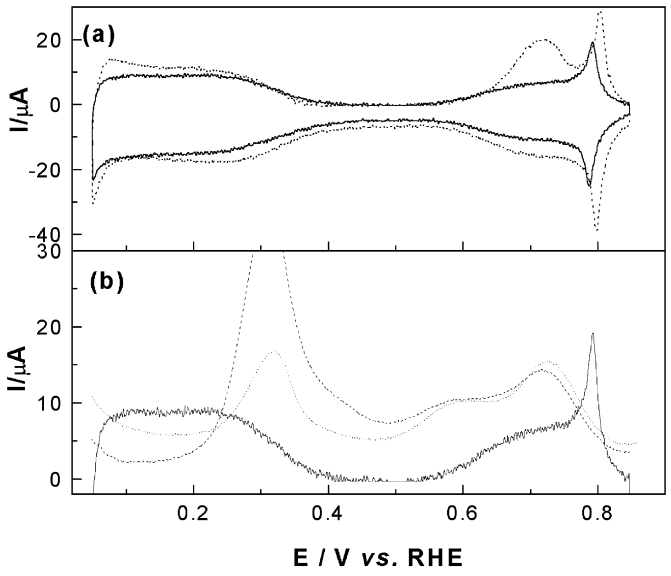

Fig. 9. Cyclic voltammetric profile of a clean Pt(111) (gray solid lines) run between 0.05 and 0.80 V at 0.10 V s^{-1} in oxygen-free 1 M sulfuric acid solution. (a) First positive-going potential scan after the CT at $E = -1.0$ V for 1 min in 1 M sulfuric acid; (b) repetitive response for Pt(111) between 0.05 and 0.80 V run at 0.10 V s^{-1} in sulfuric acid at pH = 4.0 + sodium sulfate solution (dotted lines) and first positive-going potential sweep for Pt(111) in 1 M sulfuric acid solution after 5 min of CT at $E = -2.0$ V in 1 M sulfuric acid (dashed lines).

during the application of the CT would produce molecular hydrogen from water and not from protons, which is proposed as the soluble component under peak (II). The total diffusion of base species to the bulk of the solution is completed after the potential is held at 0.05 V for more than 45 min. It has to be mentioned that after similar cathodizations on pc platinum in diluted sulfuric acid solutions of different pH's up to 4.5 (at a constant ionic force), no peak similar to that of Fig. 1 (peak (II)) was observed. However, after screening cyclic voltammetric responses of Pt(111) at different pH's, we were able to see the same large anodic peak (and also its cathodic counterpeak) contribution in the 3.5 to 5.0 pH range (see Fig. 9b, dotted lines). On the other hand, when the Pt(111) sc was polarized at $E = -2.0$ V for 5 min in the supporting electrolyte, and after the potential was held at 0.05 V for 15 min, the first positive-going potential sweep showed a voltammetric profile similar to that of the pc platinum CT treated under the same conditions (Fig. 1). Moreover, the voltammetric features are similar to those obtained on unperturbed Pt(111) at pH 4.0, but with a lower intensity in the anodic peak at 0.32 V. These results clearly demonstrate that the CT technique produces a surface rearrangement of platinum to (111) triangular sites. When the CT is applied to a Pt(111) sc and is cycled once up to 1.5 V, only the anodic peak at 0.32 V is observed, with no cathodic counterpart. The potential cycling up to these high potentials produces a fast reacidification of the platinum interface and the water discharge to hydrogen adatoms is no longer observed.

One interesting feature arises when a rotating pc platinum disc is used as the working electrode for studying the CT procedure. A reactivation is observed (for rotation rates of only 500 rpm) in scanning toward negative potentials from 1.1 V downward, exhibiting almost the same positive current profile

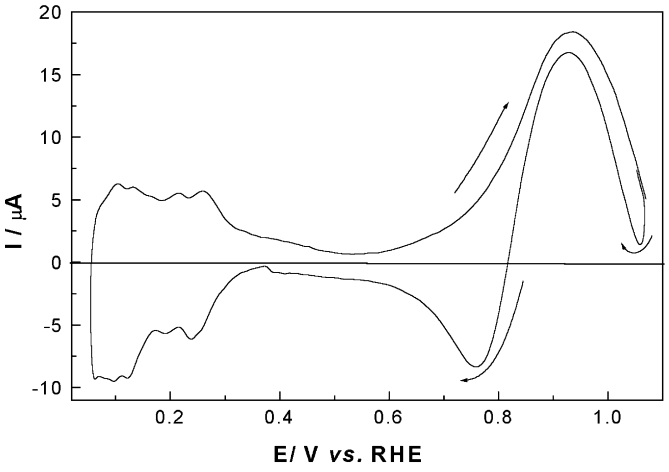

Fig. 10. First positive-going potential scan of a CT pc platinum disc (rotation rate 500 rpm) run between 0.05 and 1.10 V at 0.10 V s^{-1} in oxygen-free 1 M sulfuric acid solution. The cathodization was applied at $E = -2.0$ V for 5 min in the same solution and the excess of dissolved hydrogen was removed after holding the potential at 0.05 V for 10 min.

as that of the first anodic incursion (Fig. 10). If the same experiment is performed on a static pc platinum electrode but cycling up to 0.8 V, the same reactivation is observed. This suggests the formation of soluble platinum hydroxyl species or hydroxyl adsorbates formed at unusual lower potentials from water clusters at the interface.

We can propose different mechanisms that globally explain the results arising from CT procedures at platinum surfaces in a potential region of net hydrogen evolution. The procedure would certainly involve two main forces on a metal electrode: a large electric field created by the high electronic population on platinum at very negative cathodic potentials and a strong convective flux by molecular hydrogen evolution from platinum toward the electrolyte. The mass transport process results in an excess of surface pressure from hydrogen bubbles on (or also in) platinum, which brings up the release of the crystal lattice upon hydrogen inclusion. The result is the formation of subsurface hydrogen arising from proton electroreduction on new platinum atoms at the top layers. The existence of subsurface hydrogen on platinum has been earlier suggested by Wieckowski [75] and Martins et al. [69], proposing that the hydrogen–(subsurface) platinum species has to be electronically different from normal adsorbates. The relaxation of the crystal lattice has to occur after the surface expansion, producing platinum restructuration with hydrogen beneath. If this is so, lower-coordinated platinum species will be formed for which the interaction with water and/or hydrogen species will be fast enough to produce new features. The inclusion of molecular hydrogen rendering subsurface states into a modified opened platinum lattice is presented in Scheme 1 according to the above explanations. In mechanism 1 the reconstruction of platinum to a more opened configuration occurs after hydrogen inclusion and platinum migration to low-coordinated atoms (called "superactive") at new topmost layers. These species are able to adsorb larger amounts of hydrogen and water (or water-discharged products). The energy required to open the lattice

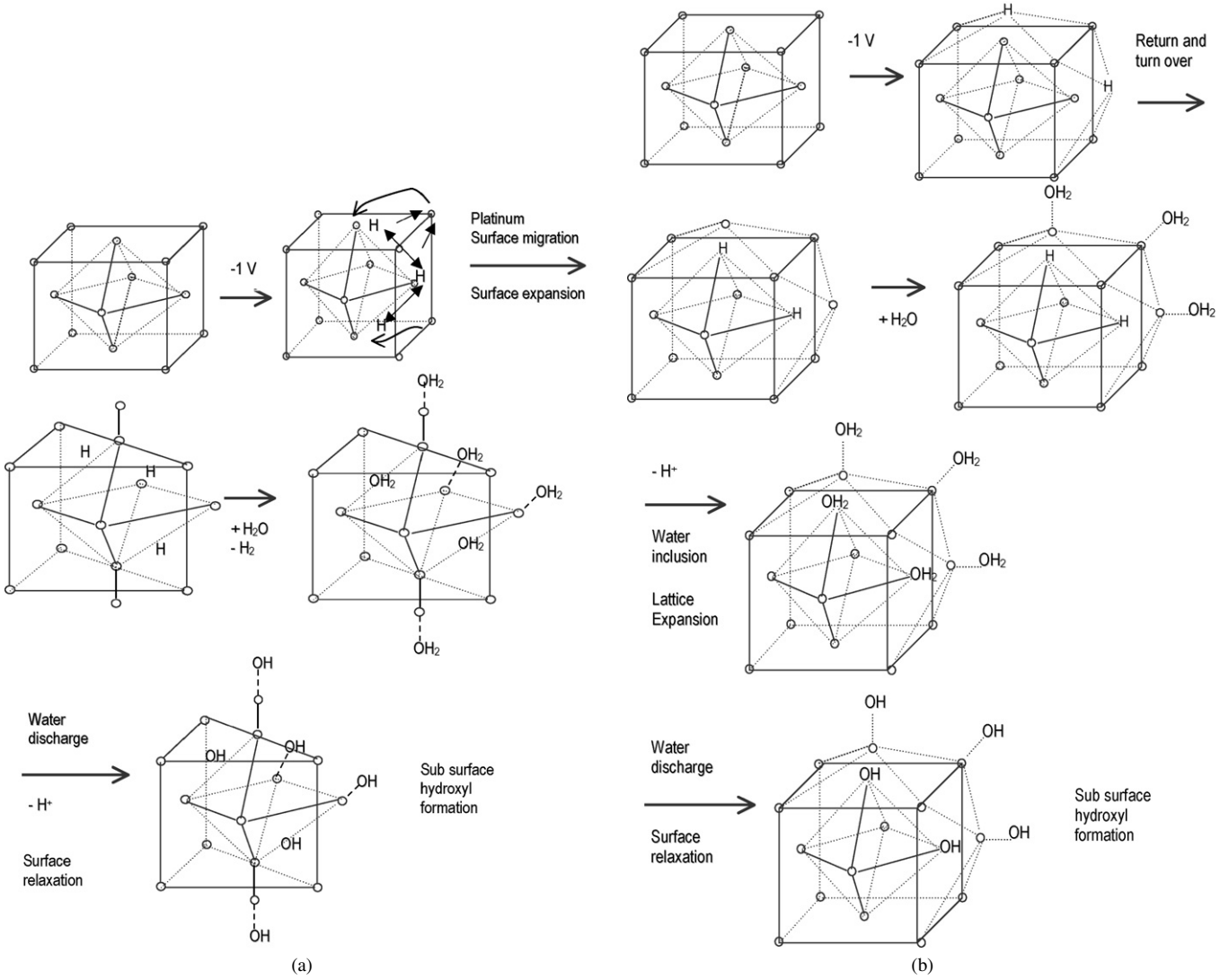

Scheme 1. Subsurface hydrogen and platinum superactive sites formed from the platinum migration mechanism or the "return and turn over" mechanism induced by cathodization. The arrows indicate the direction of migration; double arrows indicate the inner pressure caused by molecular hydrogen. (a) Mechanism 1: Platinum migration. (b) Mechanism 2: Platinum "return and turn over."

to rows or channels is obtained as explained above from mass transport mechanisms and large electronic population by the interface electric field. This process results in platinum atoms without full connection to the crystal lattice, i.e., lower coordinated platinum atoms with larger surface energy. Since the topmost layer is expanded, subsurface hydrogen is formed in the second and maybe in the third layer due to hydrogen evolution. At higher potentials, water is discharged, forming platinum/hydroxyl adsorbates and subadsorbates.

Many data on sc are available for surface expansion and crystal rearrangement processes, the effect being more noticeable on Pt(110) than on the rest of the sc's. LEED patterns on Pt(110) (1×2) [76] show no deconstruction to (1×1), since a high adsorption energy would be required to move platinum atoms from the rows. Nevertheless, hydrogen adsorption on the missing row of the (1×2) structure at hollow positions in the second layer [77] produces a 20% expansion from the topmost layer [77,78]. The formation of "subsurface hydrogen" is then likely to occur on pc platinum, in parallel with the migration of platinum atoms, yielding channels as inner $(1 \times n)$ rows. The problem of surface relaxation induced by the adsorption of hydrogen and hydroxyl adsorbates has been also studied theoretically by DFT [79] on sc clusters. On Pt(110) (1×2), experiences and calculations show that hydrogen is positioned below platinum rows [80–83]. The surface relaxation of Pt(110) (1×2) caused by hydrogen species is nearly the same as that produced by hydroxyl species, being the proposed geometry for the threefold hollow coordination.

Since the lattice expansion and surface relaxation of pc platinum are also possible, we can propose mechanism 2, assuming a "return and turn over" step after the first multicoordinated hydrogen adsorption. As a consequence of the similar effects produced by hydroxyl species on surface relaxation, this "return and turn over" can also occur with water-discharged species. Again lower coordinated platinum results with the inclusion of hydrogen beneath (subsurface hydrogen). The result is the appearance of more platinum active sites where water can be decomposed, yielding reactive hydroxyl adsorbates and subad-

sorbates. After the CT procedure, all the platinum sites have to be occupied by hydroxyl or water species in the regions at 0.9 to 1.2 V [83,84]. In this case, the formation of lower coordinated platinum produces a crystalline reorientation to triangular centers (shown in mechanism 2) that are able to explain the anomalous features found in our results in Fig. 1 from 0.5 to 0.75 V. The current vs. potential profile in this potential region has been shown to be saturated after a given E in the CT (or after lowering the value of E below −1.5 V for a preset 5 min of application time). The shape of these anodic features clearly resembles that of a true Pt(111) or a stepped plane with (111) terraces; however, when cycling up to higher potentials, the cathodic counterpart is not observed.

A complementary experiment was performed to check for these features; that is, a Pt(111) sc was treated with a CT at −1.0 V for different times from 1 to 60 min (Figs. 9a and 9b) in different pH's of sulfuric acid solution. The excess of dissolved molecular hydrogen at the interface (formed after the CT) was eliminated as explained in the Experimental section. After 1 min of CT, an increase in the broad peaks between 0.6 and 0.75 V is observed with a slight enhancement of the normal hydrogen adatoms between 0.05 and 0.35 V. When the procedure is applied for 5 min (not shown), there is a larger increase in the anodic contribution (0.6–0.75 V), but the normal hydrogen adatom desorption region is decreased to lower currents. The application of the same CT at −2.0 V for 5 min produces the appearance of a new broad peak at ca. 0.30 V as in the case of pc platinum (peak (II) in Fig. 1). However, in this case, the stirring of the solution causes the absence of this contribution. The process is then related totally to the increase in the pH at the interface as shown by Lazarescu and Clavilier [85] for Pt(111) in mildly acidified perchlorate solutions. The cyclic voltammetric response in Fig. 9b (dotted lines) for unperturbed Pt(111) sc surface at pH 4.0 corroborates these conclusions. Thus, the formation of this anodic feature on pc platinum CT at −1.5 V (or more negative values) is due to both the water discharge to hydrogen and, we also propose, the formation of subsurface hydrogen as explained above. It is likely that the most densely packed Pt(111) surface is not able to open the crystalline net or expand the surface to include hydrogen species as pc platinum under these experimental conditions.

Now we have to argue about the nature of these anodic features between 0.6 and 0.75 V, which seem to be similar to those of a true Pt(111) sc. The anomalous voltammetric behavior of a clean Pt(111) sc is dependent on the long-range order of the surface [86]. The concept of water cluster blocking and desorption in the double layer can be presented here similarly to Wagner and Ross's theory [86] for Pt(111). The concept of water clustering was proposed earlier for (111) planes and later demonstrated by STM images [87]. Strongly adsorbed hydrogen, as stated before by Clavilier et al. [88] for Pt(111), were discarded by Kolb and co-workers [89] due to the pH-independence of these peaks. The coadsorption of hydrogen and water species can be also possible. Since the charge under peaks (III) and (IV) practically remains constant at ca. 340 $\mu C\,cm^{-2}$ (exciding that of a monolayer in 100 $\mu C\,cm^{-2}$), another process has to occur, e.g., adsorbed products from the discharge of ordered water molecules. The strange nature of peaks (III) and (IV) and the saturation achieved for E values lower than −1.5 V for 5 min (as shown in Fig. 1) could also make us think of strongly bound states of hydrogen. However, when a pc platinum is treated with the CT at $E = -1$ V for less than 5 min. and then cycled up to only 0.8 V, the negative-going potential sweep shows a strong reactivation leading to the same contour as in the first positive scan. This can only occur when species existing in the bulk of the solution, or even the solvent, can react on platinum. We propose that the nature of peaks (III) and (IV) is dissociation of the hydroxyl intermediates produced from ordered water clusters on (111) or stepped planes with (111) terraces generated by the CT on pc platinum.

The specific adsorption of anions, or more properly the anodic desorption of sulfate, can also be responsible for the anomalous features of peaks (III) and (IV), as discussed by many authors. We have performed different experiments with CT applied to pc platinum with pH changes and we have found that the shape of these peaks is pH-independent. Also, when a small amount of chloride is added, the potential of peaks (III) and (IV) shifts to higher values, but the charge still remains the same. Thus, if sulfate (or bisulfate) is responsible for the anodic features, the addition of chloride has to change drastically the charge density observed in the range 0.6 to 0.75 V. Marcovic et al. [90] have demonstrated for the Pt(111)/perchloric acid interface that the addition of small amounts of chloride caused the anomalous features to shift positively and the coverage to be decreased in magnitude, indicating adsorptive displacement of the species in the anomalous peak by the strong adsorbable anion. The positive shift is consistent with the destabilization of an oxygen-type species and not to the specific adsorption of chloride. Also, the addition of base does not greatly increase the charge under peaks (III) and (IV); thus, oxygen adsorption is not the right election for the assigned adsorbed species. It is more likely that ordered water has to be responsible for the assignment.

Using Auger spectroscopy [91], it has been observed that the anodic peak at ca. 1.2 V (peak (V)) originates from the oxidation of Pt(111), but the surface species corresponding to the highly reversible peaks at 0.75 V on Pt(111) could not be identified by this ex situ technique. Since the upper limit of the potential region of peaks (III) and (IV) of our work partially coincides with the first oxygen adsorption process (onset of platinum oxidation), some form of highly activated electrosorbed oxygen also has to be considered. No adsorbed oxygen was seen by Auger spectroscopy [91] on surfaces immersed at 0.8 V; however, the possibility of nonreducible conditions is always present, so more studies would be necessary. Studies by electron spectroscopy and thermal desorption spectroscopy [91,92] have established that the oxygen species forming at 1.1 V obeys a place-exchange mechanism by hydroxyl species, so the latter has to be formed from water anodic discharge in the range 0.5–0.75 V. Ex situ spectroscopic techniques have shown that the oxygen-containing species on Pt(111) are similar to those forming on Pt(100) and pc platinum. The only difference is that the anomalous butterfly features can be structured on (111) planes such as triangular or hexagonal configurations.

The existence of two-dimensional long-range order effects is now well known in surface electrochemistry. The formation of (111) stepped planes during or after cathodization would be really surprising, but these planes were also found when platinum nanostructures were grown from amorphous oxide thin films [93] at high annealing temperatures. The appearance of a sharp reversible spike on the Pt(111)/sulfuric acid interface [94] depends on the degree of two-dimensional long-range order on the (111) domains. In this respect, on stepped platinum surfaces with (111) terraces, the sharp spike decreases as the number of rows on the terrace decreases and finally vanishes when steps are shorter than 10 atoms wide, irrespective of the step orientation [95]. A unique aspect of aqueous interfaces, which could maintain structural correlation over many molecular diameters, is the strong directional hydrogen bonding possible when water is present. It has been demonstrated that water adsorption occurs as ordered layers at cryogenic temperatures [96] under UHV as a consequence of hydrogen bonding. On a number of metal surfaces having hexagonal symmetry, such as fcc Pt(111) [97], ordered superlattices are formed, having the $(\sqrt{3} \times \sqrt{3})R30^\circ$ symmetry deduced from LEED patterns, like ice-type adlayers. Also, a description of the structure of these water superlattices on Ru(0001) was proposed [98]. LEED analysis supplemented with ESDIAD (electron-stimulated ion angular distribution) provided information about the orientation of the water molecules on the surface.

There is more evidence that adsorbed water forms a well-ordered immobile (icelike) overlayer. However, on Pt(100) [99], platinum induces only minor changes of water dynamics beyond the first layer, so down the second layer, dynamical properties are isotropic to the bulk (conclusions supported by LEED patterns). Models for the water/platinum interface have been developed using molecular dynamics [100]. It was demonstrated that the orientation ordering of water at the interface is the result of the interplay between water–water and water–platinum interactions [101]. These models are based on hard walls, Lennard-Jones walls of various powers, and polarizable walls where the polarizability tensor is described by image charges [102]. There is general agreement that the dipole vectors of water near the walls are preferentially oriented parallel to the interface and described by dipole distribution functions of an electrostatic surface potential drop. The extent of the ordering varies with the selected potentials but in most cases the polarization is small and cannot be determined easily due to statistical noise. Lee et al. [103] have shown that the orientation distribution of water dipoles and OH vectors as a function of distance from the wall can be explained by assuming a thermally disturbed ice-lattice. Sonnenschein and Heinzinger [104] have found a general preference for the parallel orientation throughout a lamina of about six layers of water molecules. Valleau and Gardner [105] assumed that six layers might be too thin in order to effectively decouple the two interfaces. However, they also found persisting orientation order in a layer of twice the thickness and even in bulk water when the final lamina configuration was used as a starting configuration. In contrast, Marchesi [106] and Aloisi et al. [107] have reported orientation isotropy with respect to the normal direction in the central part of the layer. However, it has been found that a new species forms when hydrogen and water coadsorb on various faces of platinum. The new species was identified as 'hydronium' based on electron energy loss spectroscopy (EELS) spectra and ab initio methods [108], H_5O^{2+} or H_7O^{3+} species being the most likely [106]. Theoretical calculations are able to predict a clear first-order phase transition on Pt(111) sc [109]. The principal ingredient of the theory is the assumption that water molecules in the inner Helmholtz layer are strongly oriented by the field with an important curvature of hydrogen bonds as tetrahedral configurations. The simulation of a positive polarization results in water dipoles pointing down, whereas for negative polarizations water dipoles point up. Water form a periodic structure by incorporating 1/3 of hydronium, which is adsorbed with a hydrogen down in the hollow sites of the Pt(111) electrode. Calculations assigned these features to the release of molecular hydrogen from a hydronium trimer, leaving some adsorbed anionic water complex on Pt(111) [109].

The initial step in the electrochemical generation of OH_{ads} on platinum electrodes is suggested to be not O–H bond cleavage from water over a bridge platinum site [110] but at a single platinum atom, since oxidative deprotonation of water to hydroxyl charged species exhibits low activation energies. However, in situ experimental techniques are really needed to conclude about this configuration. Iwasita and Nart [111] reported wavenumber jumps for OH stretching in adsorbed water from 3000 to 3150 cm^{-1} at 0.3 V, i.e., close to the potential of zero charge (pzc) of Pt(111)/perchloric acid (0.35 V). This shift is attributed to a change in the orientation from the H-down to the O-down configuration of water. In contrast, quite high frequencies at 3700–3600 cm^{-1} have been observed [112,113] for the O–H stretching mode on Pt(111)/sulfuric acid, in addition to drastic variations of the spectral features [112]. Thus, narrower bandwidth at more positive potentials is found, attributed to a much-ordered structure of water relative to those at negative potentials. The attenuated total reflection (ATR) method is critical to suppress the interference by bulk solution species and surface-enhanced infrared absorption spectroscopy (SEIRAS) on metal island films; this gives rise to pronounced enhancement by a factor of 10^2–10^3 compared to IRAS [114]. A strong ordering of the water molecules has been observed at potentials above pzc, in which they are partially desorbed from the surface by anion specific adsorption. Based on these results, the anodic features at peaks (III) and (IV) can be the result of either a change in the H-down to the O-down much-ordered configuration of water or a simultaneous charge transfer yielding ordered hydroxyl species [115]. In summation, the only thing that we are going to state is that during the features of peaks (III) and (IV), the transitions from disordered to ordered water (H-down to O-down) with the simultaneous oxidative formation of OH_{ads} (charged or not) is likely from CT platinum.

4.2. On the electrocatalytic consequences of cathodically treated platinum for methanol oxidation

Some studies have been conducted for carbon monoxide adsorption on a reconstructed Pt(110) (1 × 2) in acid solution [83]

using in situ X-ray scattering. The adsorption of the molecule does not induce the (1 × 2) to (1 × 1) transition observed under UHV conditions. However, a significant increase in the interatomic spacing between the first and second layers of the (1 × 2) surface occurs upon hydrogen adsorption to full coverage. The (1 × 2) surface exhibits a higher catalytic activity for carbon monoxide oxidation than the (1 × 1) surface [83].

Considering our experiments of Fig. 4, the suppressed current in the hydrogen adsorption/desorption region is more pronounced on CT than on untreated electrodes. However, methanol oxidation on CT platinum reaches a maximum at 0.85 V with current densities higher than those of untreated platinum. At this point it is appropriate to note that the small prewave peak recorded on CT surfaces develops lower currents than the reaction on bare platinum. Wieckowski et al. [116] assigned this peak to the oxidation of relatively disordered carbon monoxide coadsorbed with water, only formed when the molecule is adsorbed in the hydrogen adsorption region. Based on this observation, we can attribute this difference to the number of platinum sites capable of nucleating hydroxyl adsorbates or to the partial blocking of carbon monoxide oxidation by ordered water. The convenient equilibrium between the rate of this nucleation and the rate of methanol adsorption on the CT surface indicates that, in spite of hydroxyl and methanol adsorbates competing for the same sites, the treated surface favors methanol oxidation. Thus, the reaction rate is maximized when the coverage by each species is (nominally) the same, yielding higher current peaks for the CT treated surface at the same potential. The impedance time constant for the methanol oxidation reaction confirms these results, since comparative potential dependence values are obtained.

The methanol (or carbon monoxide adsorbate) surface configuration on CT surfaces is also important to discuss. Since we are considering the surface as a reconstructed electrode with new platinum sites and water or hydroxyl subsurface species at ca. 0.7 V, we can get a deeper insight into the surface diffusion of adsorbates on platinum. Thus, the diffusion of carbon monoxide adsorbates is two orders of magnitude faster on Pt(110) (1 × 2) than on (1 × 1) under UHV conditions [83]. An analogy between the Pt(110) (1 × 1) and the pc untreated surface can be used in this discussion. The (1 × 2) structure with opened rows can be associated with the formation of channels on a pc surface with similar mechanisms of adsorbate diffusion. Thus, we can associate the electrocatalytic effect with a faster reaction rate caused by ordered water layers on reconstructed platinum, able to oxidize with less adsorption of carbon monoxide intermediates. It seems that the higher diffusion of CO_{ads} species produces a faster reaction with OH_{ads} species in the ordered water overlayer. This means that the diffusion of the adsorbates on the CT surface will result in a higher rate for methanol oxidation.

The general scheme proposed for methanol electrooxidation on pc platinum [37–39] in acid media involves either a direct six-electron pathway or a series of several adsorption steps, some of them leading to poisoning species, prior to the final product. In the case of the CT procedure, the formation of water-oriented and hydroxyl species on superactive platinum sites, $[Pt_{superact}(OH)]$, is the main reason for the increase in the electrocatalytic activity.

$$Pt_{superact} + H_2O \leftrightarrow \left[Pt_{superact}(OH)\right] + H^+ + e^-, \tag{11}$$

together with the higher surface diffusion of CO_{ads}. The $Pt_{superact}(OH)$ species have a different energy than the normal adsorbed hydroxyl species, $[Pt(OH)]_{ad}$. However, both of them promote the oxidation of the carbon monoxide adsorbates from methanol oxidation by a direct recombination of the surface species through a Langmuir–Hinshelwood type mechanism [31]:

$$\left[Pt_{superact}(CO)\right]_{ad} + \left[Pt_{superact}(OH)\right] \rightarrow CO_2 + 2Pt_{superact} + H^- + e^-. \tag{12}$$

According to our results reaction (12) has to be faster than the common one between $[Pt(CO)]_{ad}$ and $[Pt(OH)]_{ad}$.

The oxidation of methanol on stepped or disordered platinum surfaces is guided by two major factors, the overall surface charge and the presence of adjacent water molecules from the aqueous phase. On a Pt(111) sc the methanol molecule is moved into a reactive position due to hydrogen bonds on previously adsorbed water [117]. It has been found that the methanol–water hydrogen bond on the (211) surface is strongly enhanced leading to a more exothermic methanol adsorption in comparison to the (111) plane [118]. It has been observed that the overall exothermic condition of the whole dehydrogenation "cascade" is smaller by 0.7 eV at the Pt(111)/water interface than at the Pt(111)/vacuum interface, clearly showing the influence of preadsorbed water [119,120]. This fact has been explained by hydrogen-bond stabilization of the complex state and weakening of the water–platinum interaction. Water molecules adsorbed onto platinum in acid solutions vibrate at ca. 3500 and 3000–3100 cm^{-1}, but change to a new O–H stretching vibration at 3658 cm^{-1} by interaction with neighbor adsorbed species (such as carbon monoxide from methanol) [121]. In situ ATR-SEIRAS shows that the newly adsorbed water coexists with adsorbed carbon monoxide derived from methanol. Its consumption during oxidation varies linearly with the intensity of both adsorbed water and linear carbon monoxide. This is a strong proof that the water molecules coexist with the resultant carbon monoxide and are the species directly reacting with carbon monoxide, promoting further methanol oxidation [122]. The change in the structure of the interfacial water layer brought about by methanol adsorption is responsible for the difference between the experimentally determined pzc of the CO-covered Pt(111), 1.10 V, and the estimated potential of zero free charge of clean Pt(111), 0.23 V. From these values it has been calculated that the average angle between the dipole moment of water and the platinum surface, at room temperature and at the pzc, decreases from 7.85° for clean Pt(111) to 1.46° for the CO-covered Pt(111) [123].

Chang and Weaver [124] found that coadsorption of water at lower carbon monoxide coverages on Pt(111) in the electrochemical environment favors CO_{ads} binding in bridging sites. Vibration frequencies for both linear and bridging geometries at high coverages are at least 20–30 cm^{-1} lower in the electrochemical than UHV conditions. These environmental effects

upon the CO_{ads} binding suggest that the double-layer effects are determining in the first stages of electrocatalytic anodic reactions. On the other hand, the same important interaction between water and CO_{ads} has been observed using in situ IRAS and STM [125]. Carbon monoxide adsorbed on Pt(111) at 0.4 V shows a strong interaction with overlayer water molecules and retarded the oxidation to carbon dioxide, whereas adsorption at 0.05 V started to oxidize at lower potentials. However, It has been also reported [126] using quantum-chemical and ab initio molecular dynamics that the oxidation of methanol starts by the formation of a hydrogen bond from the OH group of methanol with a solvent molecule. The initial step of the reaction is the cleavage of a CH bond which points toward the platinum surface. Geometry optimizations of methanol molecules in the absence of water show physisorbed methanol more stable via the oxygen than via the methyl end of the molecule.

Summing up, our results and those previously obtained by other authors show that the newly adsorbed water (on lower coordinated platinum) coexists with adsorbed carbon monoxide from methanol. This explains the catalytic effect for methanol oxidation through the formation of new intermediates; that is, $[Pt_{superact}(CO)]_{ad}$ and $[Pt_{superact}(OH)]$, in the range 0.6–0.75 V.

5. Conclusions

The cathodization method produces new active platinum states defined as lower coordinated platinum atoms, not available on polycrystalline electrodes in an aqueous solution. They are related to the formation of subsurface hydrogen species and hydroxyl adsorbates (or partially discharged ordered water molecules) on lower coordinated platinum, according to platinum migration and hydrogen inclusion mechanisms.

Repetitive and stable conditions were found in the range 0.5–0.75 V, where the electrocatalytic activity of these new surfaces toward methanol oxidation was compared with untreated electrodes by electrochemical impedance spectroscopy, chronoamperometry, and cyclic voltammetry.

The cathodic procedure enhances the methanol oxidation current peaks with charge densities values higher than on untreated platinum. The integration of chronoamperometric plots in methanol acid media presents the largest difference in the 0.6–0.7 V region with respect to the original surface. The values of polarization resistance for methanol oxidation on the cathodic-treated platinum are lower than those of the original surface. According to the time constant values for methanol oxidation, the original surface can be considered as less tolerant to the formation of catalytic poisons.

Acknowledgments

The authors thank the PDT 16/02 Project for financial support. C.F.Z. is a researcher at PEDECIBA/United Nations. The authors specially thank Prof. Dr. S. Bonilla for helpful discussion and comments on the paper.

References

[1] L.D. Burke, M.E.G. Lyons, in: R.E. White, J.O'M. Bockris, B.E. Conway (Eds.), Modern Aspects of Electrochemistry, vol. 18, Plenum, New York, 1986, pp. 169–248.
[2] B.E. Conway, G. Jerkiewicz, J. Electroanal. Chem. 339 (1992) 123.
[3] M. Farebrother, M. Goledzinowski, G. Thomas, V. Birss, J. Electroanal. Chem. 297 (1991) 469.
[4] V. Birss, M. Goledzinowski, J. Electroanal. Chem. 351 (1993) 435.
[5] V.I. Birss, M. Chang, J. Segal, J. Electroanal. Chem. 355 (1993) 181.
[6] S.J. Xia, V.I. Birss, Electrochim. Acta 45 (2000) 3659.
[7] S.H. Kim, K.C. Kim, Y.S. Kim, H.J. Kim, Curr. Appl. Phys. 6 (2006) 1036.
[8] M. Goto, A. Kasahara, M. Tosa, Vacuum 80 (2006) 740.
[9] B.J. Jianga, T.J. Jianga, C.X. Rena, X.H. Liua, X. Wanga, T. Fenga, Z.X. Zhanga, Z.T. Songa, L.P. Zheng, Thin Solid Films 483 (2005) 411.
[10] T. Kikuchi, H. Takahashi, T. Maruko, Electrochim. Acta 52 (2007) 2352.
[11] G.-Y. Zhao, C.-L. Xu, D.-J. Guo, H. Li, H.-L. Li, Appl. Surf. Sci. 253 (2007) 3242.
[12] E. Aschauer, R. Fasching, M. Varahram, G. Jobst, G. Urban, G. Nicolussi, W. Husinsky, G. Friedbacher, M. Grasserbauer, J. Electroanal. Chem. 426 (1997) 157.
[13] A.C. Chialvo, W.E. Triaca, A.J. Arvia, J. Electroanal. Chem. 146 (1983) 93.
[14] A.J. Arvia, R.C. Salvarezza, W.E. Triaca, Electrochim. Acta 34 (1989) 1057.
[15] S. Zhuo, K. Sohlberg, Physica B 381 (2006) 12.
[16] L.D. Burke, J.A. Collins, M.A. Horgan, L.M. Hurley, A.P. O'Mullane, Electrochim. Acta 45 (2000) 4127.
[17] L.D. Burke, L.M. Hurley, Electrochim. Acta 44 (1999) 3451.
[18] L.D. Burke, J.A. Collins, M.A. Murphy, J. Solid State Electrochem. 4 (1999) 34.
[19] L.D. Burke, G.M. Bruton, J.A. Collins, Electrochim. Acta 44 (1998) 1467.
[20] L.D. Burke, Electrochim. Acta 39 (1994) 1841.
[21] G. Lang, K.E. Heusler, J. Electroanal. Chem. 377 (1994) 1.
[22] A.W. Adamson, I. Ling, Adv. Chem. Ser. 43 (1964) 59.
[23] A.N. Frumkin, in: P. Delahay (Ed.), Advances in Electrochemistry and Electrochemical Engineering, vol. 3, Interscience, New York, 1963, pp. 287–391.
[24] W.M. Vogel, J.M. Baris, Electrochim. Acta 23 (1978) 463.
[25] S.J. Clouser, J.C. Huang, E. Yeager, J. Appl. Electrochem. 23 (1993) 597.
[26] A. Jaccoud, G. Fóti, C. Comninellis, Electrochim. Acta 51 (2006) 1264.
[27] H. Matsuhashi, S. Nishiyama, H. Miura, K. Eguchi, K. Hasegawa, Y. Iizuka, A. Igarashi, N. Katada, J. Kobayashi, T. Kubota, T. Mori, K. Nakai, N. Okazakim, M. Sugioka, T. Umekio, Y. Yazawa, D. Lu, Appl. Catal. A Gen. 272 (2004) 329.
[28] M. Marwood, C.G. Vayenas, J. Catal. 178 (1998) 429.
[29] S. Bebelis, N. Kotsionopoulos, Solid State Ionics 177 (2006) 2205.
[30] C.-C. Changa, T.-C. Wen, Electrochim. Acta 52 (2006) 623.
[31] T. Iwasita, F.C. Nart, W. Vielstich, Ber. Bunsenges. Phys. Chem. 94 (1990) 1030.
[32] H. Gasteiger, N. Markovic, P. Ross, E. Cairns, J. Phys. Chem. 97 (1993) 12020.
[33] H. Gasteiger, N. Markovic, P. Ross, E. Cairns, J. Electrochem. Soc. 141 (1994) 1795.
[34] N. Markovic, H. Gasteiger, P.N. Ross, I. Villegas, M. Weaver, J. Electrochim. Acta 40 (1995) 91.
[35] C.F. Zinola, S. Martinez, J. Solid State Electrochem. Special Issue (2007), in press.
[36] W. Chrzanowski, A. Wieckowski, Langmuir 14 (1998) 1967.
[37] M. Krausa, W. Vielstich, J. Electroanal. Chem. 379 (1994) 307.
[38] M. Hogarth, J. Munk, A. Shukla, A. Hammnett, J. Appl. Electrochem. 24 (1994) 85.
[39] W. Chrzanowski, H. Kim, A. Wieckowski, Catal. Lett. 50 (1998) 69.
[40] C. Coutanceau, A. Ralotondrainibé, A. Lima, E. Garnier, S. Pronier, J. Léger, C. Lamy, J. Appl. Electrochem. 34 (2004) 61.
[41] E. Spinacé, A. Neto, M. Linardi, J. Power Sources 129 (2004) 121.
[42] S.H. Bonilla, C.F. Zinola, J. Rodriguez, V. Diaz, M. Ohanian, S. Martinez, B. Gianetti, J. Colloid Interface Sci. 288 (2005) 377.

[43] S. Strbac, C. Johnston, G. Lu, A. Crown, A. Wieckowski, Surf. Sci. 573 (2004) 80.
[44] V. Colle, M. Giz, G. Tremiliosi Filhio, J. Braz. Chem. Soc. 14 (2003) 601.
[45] S. Strbac, R.J. Behm, A. Crown, A. Wieckowski, Surf. Sci. 517 (2002) 2078.
[46] P.A. Thiel, T.E. Madey, Surf. Sci. Rep. 7 (1987) 211.
[47] N.M. Marković, P.N. Ross Jr., Surf. Sci. Rep. 45 (2002) 117.
[48] S.R. Brankovic, J. McBreen, R.R. Adzic, J. Electroanal. Chem. 503 (2001) 99.
[49] S.T. Kuk, A. Wieckowski, J. Power Sources 141 (2005) 1.
[50] F. Vigier, C. Coutanceau, A. Perrard, E.M. Belgsir, C. Lamy, J. Appl. Electrochem. 34 (2004) 439.
[51] A. Neto, M. Giz, J. Perez, E.A. Ticianelli, E.R. Gonzalez, J. Electrochem. Soc. 149 (2002) A272.
[52] H. Liu, C. Song, L. Zhang, J. Zhang, H. Wang, D.P. Wilkinson, J. Power Sources 155 (2006) 95.
[53] C.T. Hable, M.S. Wrighton, Langmuir 9 (1993) 3284.
[54] K. Wang, H.A. Gasteiger, N.M. Markovic, P.N. Ross Jr., Electrochim. Acta 41 (1996) 2587.
[55] W.T. Napporn, H. Laborde, J.-M. Lèger, C. Lamy, J. Electroanal. Chem. 404 (1996) 153.
[56] Y. Morimoto, E.B. Yeager, J. Electroanal. Chem. 444 (1998) 95.
[57] A.N. Golikand, S.M. Golabi, M.G. Maragheh, L. Irannejad, J. Power Sources 145 (2005) 116.
[58] T. Kim, K. Kobayashi, M. Takahashi, M. Nagai, Chem. Lett. 34 (2005) 798.
[59] A. Neto, R. Dias, M.M. Tusi, M. Linardi, E.V. Spinacé, J. Power Sources 166 (2007) 87.
[60] Z.-B. Wang, G.-P. Yin, P.-F. Shi, B.-Q. Yang, P.-X. Feng, J. Power Sources 166 (2007) 317.
[61] L. Zhang, K. Lee, J. Zhang, Electrochim. Acta 52 (2007) 3088.
[62] Z. Liu, M. Shamsuzzoha, E. Ada, W.M. Reichert, D.E. Nikles, J. Power Sources 164 (2007) 472.
[63] J. Zhu, Y. Su, F. Cheng, J. Chen, J. Power Sources 166 (2007) 331.
[64] I.-S. Park, K.-S. Lee, D.-S. Jung, H.-Y. Park, Y.-E. Sung, Electrochim. Acta 52 (2007) 5599.
[65] C. Xu, L. Cheng, P. Shen, Y. Liu, Electrochem. Commun. 9 (2007) 997.
[66] I.-S. Park, K.-W. Park, J.-H. Choi, C.R. Park, Y.-E. Sung, Carbon 45 (2007) 28.
[67] J. Clavilier, J. Electroanal. Chem. 107 (1980) 211.
[68] J. Clavilier, D. Armand, J. Electroanal. Chem. 199 (1986) 187.
[69] M.E. Martins, C.F. Zinola, G. Andreasen, R.C. Salvarezza, A.J. Arvia, J. Electroanal. Chem. 445 (1998) 135.
[70] J. Willsau, O. Wolter, J. Heitbaum, J. Electroanal. Chem. 185 (1985) 163.
[71] J.P. Hoare, Electrochim. Acta 26 (1981) 225;
J.P. Hoare, Electrochim. Acta 27 (1982) 1751.
[72] C. Gabrielli, M. Keddam, Electrochim. Acta 41 (1996) 957.
[73] G.J. Brug, A.L.G. van den Eeden, M. Sluyters-Rehbach, J.H. Sluyters, J. Electroanal. Chem. 176 (1984) 275.
[74] R.E. Melnick, G.T.R. Palmore, J. Phys. Chem. B 105 (2001) 1012.
[75] A. Wieckowski, J. Chim. Phys. 88 (1991) 1247.
[76] W.T. Lee, L. Ford, P. Blowers, H.L. Nigg, R.I. Masel, Surf. Sci. 416 (1998) 141.
[77] E. Kirsten, G. Parschau, W. Stocker, K.H. Rieder, Surf. Sci. Lett. 231 (1990) L183.
[78] R.A. Olsen, G.J. Kroes, E.J. Baerends, J. Chem. Phys. 111 (1999) 11155.
[79] N.M. Markovič, B.N. Grgur, C.A. Lucas, P.N. Ross, Surf. Sci. 384 (1997) L805.
[80] R.J. Nichols, in: J. Lipkowski, P.N. Ross (Eds.), Frontiers of Electrochemistry, Wiley–VCH, New York, 1999, p. 99.
[81] A. Peremans, A. Tadjeddine, J. Chem. Phys. 103 (1995) 7197.
[82] A. Tadjeddine, A. Peremans, J. Electroanal. Chem. 409 (1996) 115.
[83] M.T.M. Koper, R.A. van Santen, J. Electroanal. Chem. 476 (1999) 64.
[84] K. Bedurftig, S. Volkening, Y. Wang, J. Winterline, K. Jacoby, G. Ertl, J. Chem. Phys. 111 (1999) 11147.
[85] V. Lazarescu, J. Clavilier, Electrochim. Acta 44 (1998) 931.
[86] F.T. Wagner, P.N. Ross, J. Electroanal. Chem. 250 (1988) 301.
[87] K. Itaya, S. Sugarawa, K. Sashikata, N. Furuya, J. Vac. Sci. Technol. A 8 (1990) 515.
[88] J. Clavilier, D. Armand, B.L. Wu, J. Electroanal. Chem. 135 (1982) 159.
[89] K. Al-Jaaf-Golze, D.M. Kolb, D. Scherson, J. Electroanal. Chem. 200 (1986) 353.
[90] M. Markovic, M. Hanson, G. McDougall, E. Yeager, J. Electroanal. Chem. 214 (1986) 555.
[91] F.T. Wagner, P.N. Ross Jr., Appl. Surf. Sci. 24 (1985) 87.
[92] M. Peuckert, F.P. Coenen, H.P. Bonzel, Electrochim. Acta 29 (1984) 1305.
[93] S.H. Kim, K.C. Kim, Y.S. Kim, H.J. Kim, Curr. Appl. Phys. 6 (2006) 1036.
[94] B. Alvarez, J.M. Feliu, J. Clavilier, Electrochem. Commun. 4 (2002) 379.
[95] J. Clavilier, K. El Achi, A. Rodes, Chem. Phys. 141 (1990) 1.
[96] P. Thiel, T. Madey, Surf. Sci. Rep. 7 (1988) 211.
[97] G.B. Fisher, J.L. Gland, Surf. Sci. 94 (1980) 446.
[98] D. Doering, T. Madey, Surf. Sci. 123 (1982) 305.
[99] H. Ibach, S. Lehwald, Surf. Sci. 91 (1980) 187.
[100] E. Spohr, J. Phys. Chem. 93 (1989) 6171.
[101] E. Spohr, Chem. Phys. 141 (1990) 87.
[102] E. Spohr, K. Heinzinger, Electrochim. Acta 33 (1988) 1211.
[103] C.Y. Lee, J.A. McCammon, P.J. Rossky, J. Chem. Phys. 80 (1984) 4448.
[104] R. Sonnenschein, K. Heinzinger, Chem. Phys. Lett. 102 (1983) 550.
[105] J.P. Valleau, A.A. Gardner, J. Chem. Phys. 86 (1987) 4162.
[106] M. Marchesi, Chem. Phys. Lett. 97 (1983) 224.
[107] G. Aloisi, R. Guidelli, R.A. Jackson, S.M. Clark, P. Barnes, J. Electroanal. Chem. 206 (1986) 131.
[108] N. Chen, P. Blowers, R.I. Masel, Surf. Sci. 419 (1999) 150.
[109] L. Blum, D.A. Huckaby, N. Marzari, R. Car, J. Electroanal. Chem. 537 (2002) 7.
[110] A.B. Anderson, N.M. Neshev, R.A. Sidik, P. Shiller, Electrochim. Acta 47 (2002) 2999.
[111] T. Iwasita, F.C. Nart, Prog. Surf. Sci. 55 (1997) 271.
[112] Y. Shingaya, M. Ito, Surf. Sci. 386 (1997) 34.
[113] K. Ataka, M. Osawa, Langmuir 14 (1998) 951.
[114] M. Osawa, Top. Appl. Phys. 81 (2001) 163.
[115] F.T. Wagner, P.N. Ross Jr., Surf. Sci. 160 (1985) 305.
[116] A. Wieckowski, M. Rubel, C. Gutiérrez, J. Electroanal. Chem. 382 (1995) 97.
[117] C. Hartnig, E. Spohr, Chem. Phys. 319 (2005) 185.
[118] C. Hartnig, J. Grimminger, E. Spohr, Electrochim. Acta 52 (2007) 2236.
[119] R. Paul, S.J. Paddison, Phys. Rev. E 67 (2003) 16108.
[120] Y. Okamoto, O. Sugino, Y. Mochizuki, T. Ikeshoji, Y. Morikawa, Chem. Phys. Lett. 377 (2003) 236.
[121] H. Shiroishi, Y. Ayato, K. Kunimatsu, T. Okada, J. Electroanal. Chem. 581 (2005) 132.
[122] A. Cuesta, J. Electroanal. Chem. 587 (2006) 329.
[123] A. Cuesta, Surf. Sci. 572 (2004) 11.
[124] S.-C. Chang, M.J. Weaver, Surf. Sci. 238 (1990) 142.
[125] K. Yoshimi, M.-B. Song, M. Ito, Surf. Sci. 368 (1996) 389.
[126] C. Hartnig, E. Spohr, Chem. Phys. 319 (2005) 185.